JOC Article

Unsymmetric Pyrrole, Thiophene, and Furan-Conjugated Comonomers Prepared Using Azomethine Connections: Potential New Monomers for Alternating Homocoupled Products

Stéphane Dufresne and W. G. Skene*

Département de Chimie, Pavillon J. A. Bombardier, Université de Montréal, CP 6128, succ. Centre-ville, Montréal, Québec, Canada H3C 3J7

w.skene@umontreal.ca

Received January 30, 2008

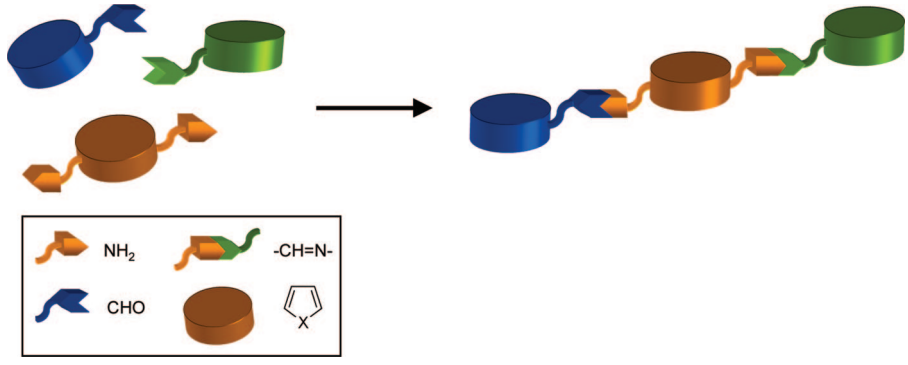

Unsymmetric comonomers consisting of thiophene, pyrrole, and furan heterocycles were prepared using azomethine bonds. Photophysical investigation of the novel π-donor−donor−donor segmented compounds revealed that their singlet excited state is only partially deactivated by internal conversion unlike their all-thiophene azomethine analogues. Temperature-dependent steady-state and time-resolved emission studies demonstrated that the unsymmetric compounds deactivated efficiently their singlet excited state by intersystem crossing to populate the triplet manifold. This lower energy state is rapidly deactivated by nonradiative self-quenching. The comonomers and their anodically prepared conjugated homocoupled products are both electrochemically active, resulting in new compounds that can be mutually oxidized and reduced. Meanwhile, the oxidation potentials of the coupled products are shifted by up to 400 mV to more cathodic potentials relative to their corresponding comonomers, confirming their increased degree of conjugation.

Introduction

Conjugated materials such as phenylvinylenes have found many applications as functional materials because of their interesting photophysical and electrochemical properties. Many potential applications for such materials include light emitting diodes,[1–8] solar cells,[9–11] field effect transistors,[12–14] and molecular sensors.[15] Even though π-conjugated materials are successfully prepared by well-established protocols, including Wittig coupling,[16,17] the products must be extensively purified

(1) Veinot, J. G. C.; Marks, T. J. *Acc. Chem. Res.* **2005**, *38*, 632–643.
(2) Perepichka, I. F.; Perepichka, D. F.; Meng, H.; Wudl, F. *Adv. Mater.* **2005**, *17*, 2281–2305.
(3) Leclerc, M. *J. Polym. Sci. Part A: Polym. Chem.* **2001**, *17*, 2867–2873.
(4) Williams, E. L.; Haavisto, K.; Li, J.; Jabbour, G. E. *Adv. Mater.* **2007**, *19*, 197–202.
(5) Parthasarathy, G.; Liu, J.; Duggal, A. R. *Electrochem. Soc. Interface* **2003**, *12*, 42–47.
(6) Mitschke, U.; Bauerle, P. *J. Mater. Chem.* **2000**, *10*, 1471–1507.
(7) Kraft, A.; Grimsdale, A. C.; Holmes, A. B. *Angew. Chem., Int. Ed.* **1998**, *37*, 402–428.
(8) Ton-That, C.; Stockton, G.; Phillips, M. R.; Nguyen, T.-P.; Huang, C. H.; Cojocaru, A. *Polym. Int.* **2008**, *57*, 496–501.
(9) Gratzel, M. M.; Jacques, E. *Electron Transfer Chem.* **2001**, 589–644.
(10) Segura, J. L.; Martín, N.; Guldi, D. M. *Chem. Soc. Rev.* **2005**, *34*, 31–47.
(11) Smith, G. B. *Sol. Energy Mater. Sol. Cells* **2004**, *84*, 395–409.
(12) Horowitz, G. *Adv. Mater.* **1998**, *10*, 365–377.
(13) Katz, H. E.; Dodabalapur, A.; Bao, Z. In *Handbook of Oligo- and Polythiophenes*; Fichou, D., Ed.; Wiley-VCH: Weinheim, Germany, 1999; pp 459−489.
(14) Kraft, A. *Chem. Phys. Chem.* **2001**, *2*, 163–165.
(15) Mikroyannidis, J. A.; Barberis, V. P. *J. Polym. Chem. Part A: Polym. Chem.* **2007**, *45*, 1481–1491.
(16) Hu, Z.-Y.; Fort, A.; Barzoukas, M.; Jen, A. K. Y.; Barlow, S.; Marder, S. R. *J. Phys. Chem. B* **2004**, *108*, 8626–8630.
(17) Turbiez, M.; Frere, P.; Roncali, J. *Tetrahedron* **2005**, *61*, 3045–3053.

10.1021/jo8002503 CCC: $40.75
Published on Web 04/15/2008

SCHEME 1. Representation of Potential Product Distribution for a Three-Component Reaction of Vinylene and Azomethine Formation Prepared by Wittig and Azomethine Condensation Reactions, Respectively

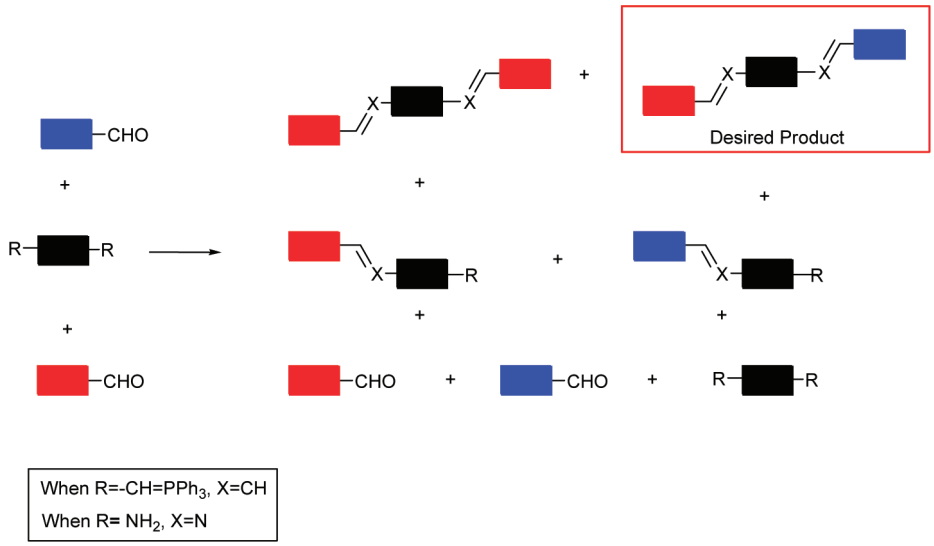

in order to remove undesired byproduct. For example, with Wittig coupling, triphenylphosphine oxide accounts for a considerable amount of the product obtained, and it also leads to inconsistent properties in the final products if it is not thoroughly removed. Similar inconsistent properties occur with anodically prepared polymers[18–20] owing to uncontrollable competing side reactions such as α,β-coupling, over oxidation, and cross-linking defects. Comparable defects can also occur with the electrochemical preparation of alternating copolymers owing to mismatched oxidation potentials of the different monomers. Consequently, the oxidation potentials of the two monomers to be copolymerized must be similar in order to suppress homopolymerization and other undesired defects. An appropriate solution to these problematic electrochemical shortcomings involves the use of comonomers. These are monomers containing the elements of the copolymer structure consisting of a central aromatic core sandwiched between external aryl groups. Such an arrangement offers the possibility to suppress polymer defects that would otherwise limit the degree of conjugation leading to incompatible properties for uses as functional materials.[21–23]

Despite the synthetic advantages of using comonomers for the anodic preparation of conjugated polymers, their synthesis involves challenging coupling reactions and they also suffer from problematic purifications. Additionally, unsymmetric π-rich or π-poor comonomers desired for controlling the spectroscopic and electrochemical properties are difficult to prepare in high yields by these protocols (vide supra).[24,25] Given the potential enhanced property tailoring that is possible with unsymmetric comonomers, new and efficient methods for the synthesis of such comonomers are therefore required.

Coupling of complementary aryl aldehydes and amines affording azomethines (−*N*═CH−) is an ideal alternative for the synthesis of conjugated comonomers. Azomethines are isoelectronic to their C═C vinylene analogues, and mild reaction conditions are required for their synthesis involving simple purifications when necessary. Unlike conventional coupling techniques that give a mixture of products when using a three-component reaction depicted in Scheme 1, selective product formation affording unsymmetric products is possible with azomethines by controlling the reagent stoichiometry and solvents.[26,27] The result of the self-assembly between the two complementary aryl groups is a robust bond exhibiting high hydrolytic, oxidative, and reductive resistance.[26–28]

To address the synthetic challenge of unsymmetric conjugated comonomers consisting of various heterocycles, we used the stable diaminothiophene **1** for preparing the novel azomethines reported in Scheme 2. This heterocycle is an ideal compound to use as a core for comonomer synthesis because it possesses a low oxidation potential, which when incorporated into a comonomer is ideal for anodic coupling. This eliminates the risk of undesired decomposition products that are otherwise produced with monomers possessing high oxidation potentials. Additionally, **1** is air-stable, and condensation with aryl aldehydes is achieved easily, affording stable conjugated comonomers, which are capable of sustaining anodic polymerization. Our previous successful comonomer synthesis[26–31] and our ongoing conjugated azomethines research have prompted us to prepare a new series of unsymmetric π-rich heterocyclic comonomers consisting of thiophenes, pyrroles, and furans and to investigate their physical properties. These new π-donor−donor−donor compounds and their anodically produced polymers are of particular interest because they are expected to exhibit enhanced properties relative to homoaryl azomethines.

(18) Jenkins, I. H.; Rees, N. G.; Pickup, P. G. *Chem. Mater.* **1997**, *9*, 1213–1216.
(19) Hughes, G.; Bryce, M. R. *J. Mater. Chem.* **2005**, *15*, 94–107.
(20) Moliton, A.; Hiorns, R. C. *Polym. Int.* **2004**, *53*, 1397–1412.
(21) Ng, S. C.; Chan, H. S. O.; Wong, P. M. L.; Tan, K. L.; Tan, B. T. G. *Polymer* **1998**, *39*, 4963–4968.
(22) Yang, C.-J.; Jenekhe, S. A. *Macromolecules* **1995**, *28*, 1180–1196.
(23) Thomas, O.; Inganäs, O.; Andersson, M. R. *Macromolecules* **1998**, *31*, 2676–2678.
(24) Hansford, K. A.; Guarin, S. A. P.; Skene, W. G.; Lubell, W. D. *J. Org. Chem.* **2005**, *70*, 7996–8000.
(25) Dufresne, S.; Hanan, G. S.; Skene, W. G. *J. Phys. Chem. B* **2007**, *111*, 11407–11418.
(26) Bourgeaux, M.; Pérez Guarin, S. A.; Skene, W. G. *J. Mater. Chem.* **2007**, *17*, 972–979.
(27) Pérez Guarìn, S. A.; Bourgeaux, M.; Dufresne, S.; Skene, W. G. *J. Org. Chem.* **2007**, *72*, 2631–2643.
(28) Dufresne, S.; Bourgeaux, M.; Skene, W. G. *J. Mater. Chem.* **2007**, *17*, 1166–1177.
(29) Bourgeaux, M.; Skene, W. G. *Macromolecules* **2007**, *40*, 1792–1795.
(30) Pérez Guarìn, S. A.; Dufresne, S.; Tsang, D.; Sylla, A.; Skene, W. G. *J. Mater. Chem.* **2007**, *17*, 2801–2811.
(31) Pérez Guarìn, S. A.; Skene, W. G. *Mater. Lett.* **2007**, *61*, 5102–5106.

SCHEME 2. Azomethines Examined[a]

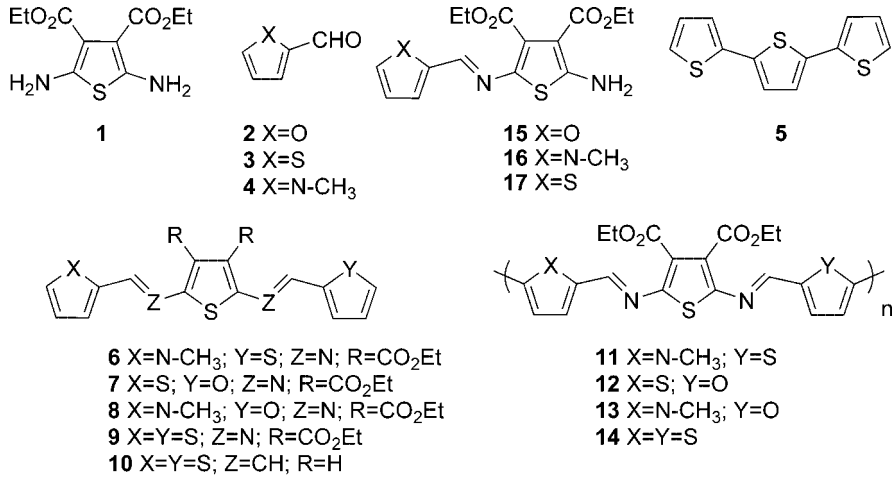

[a] Their precursors and their corresponding products are obtained by anodic coupling. For simplicity, **11**−**14** are illustrated as *head-to-tail* products even though a mixture of *head-to-tail* and *head-to-head* regioregular products are expected.

For example, mutual oxidation and reduction leading to p- and n-doping of the azomethine comonomers is expected contrary to their oligothiophene and thiophene vinylene analogues that are predominately p-doped.

Even though **1** has been known since the early 70s,[32,33] its challenging preparation and low yields preclude it as a suitable precursor for the preparation of azomethines. Subsequently, diamino precursors required for azomethine preparation have been limited to phenylene diamine and its derivatives. Such homoaryl precursors are problematic because they decompose under ambient conditions while their azomethine products are highly insoluble.[22,34–36] Moreover, they suffer from unwanted oxidative decomposition, and conjugated polymers produced anodically by α−α homocoupling are rarely obtained.[21,37] The properties of the homoaryl azomethine are also incompatible with functional materials, and as a result, azomethines have attracted little attention.[23,38,39] Our recent simple scale-up preparation of **1**[26–29,40] concomitant with its optimized condensation for the preparation of novel azomethines consisting uniquely of thiophenes has renewed the interest in azomethines as functional materials. Given the importance of assessing the compatibility of these new compounds as functional materials, we examined the structure−property relationship of novel unsymmetric heterocyclic conjugated azomethines. Herein, we present the preparation of novel π-rich comonomers along with their photophysics and redox properties including their anodically coupled products.

Results and Discussion

Preparation. The diaminothiophene core (**1**) required for the condensation with heteroaldehydes **2**−**4** was obtained in large quantities by a modified one-pot Gewald[32,40] batch reaction using inexpensive ethylcyanoacetate and elemental sulfur. The electron-withdrawing ester in the 3 and 4 positions deactivates the electron-rich amines, conferring a high degree of stability to **1** under ambient conditions. In contrast, its electron-rich unsubstituted analogue cannot be isolated, and it spontaneously decomposes under ambient conditions. The azomethine formed when condensing an arylaldehyde with **1** is also electron-withdrawing, and it further reduces the reactivity of the remaining terminal amine in monoazomethine compounds such as **15**−**17**. More stringent reaction conditions are therefore required to induce the second condensation for the preparation of bisazomethines such as the unsymmetric comonomers reported in Scheme 2. The change in amine reactivity provides a versatile means to prepare **6**−**8** in a stepwise manner from the corresponding monoazomethines **15**−**17**. The required monoazomethines were obtained by refluxing 1 equiv of the arylaldehyde with **1**. The selectivity for monoaddition to afford uniquely the corresponding monoazomethines is apparent from the reaction yields. An unselective reaction affording a mixture of monoazomethine and symmetric bisazomethines would otherwise lead to low product yields. The unsymmetric bisazomethines were prepared with 1 equiv of the corresponding aldehyde, which was activated with $TiCl_4$ and then combined with either **15**, **16**, or **17** in refluxing toluene. The bisazomethine products obtained in good yields confirm the robustness of the azomethine, while weak azomethine linkages would decompose under the reaction conditions used. The stability of the comonomers is further evidenced by the absence of exchange products involving Lewis acid mediated aldehyde exchange.[28,41,42] The differential reactivity notwithstanding, the order in which the aldehydes must be reacted in order to obtain the final comonomers had to be carefully chosen. For example, **7** and **8** could only be prepared from the furan azomethine **15**, while **6** could

(32) Gewald, V. K.; Kleinert, M.; Thiele, B.; Hentschel, M. *J. Prak. Chem.* **1972**, *314*, 303–314.
(33) Gewald, K.; Gruner, M.; Hain, U.; Süptitz, G. *Monatsh. Chem.* **1988**, *119*, 985–992.
(34) Yang, C.-J.; Jenekhe, S. A. *Chem. Mater.* **1991**, *3*, 878–887.
(35) Suematsu, K.; Nakamura, K.; Takeda, J. *Colloid Polym. Sci.* **1983**, *261*, 493–501.
(36) Morgan, P. W.; Kwolek, S. L.; Pletcher, T. C. *Macromolecules* **1987**, *20*, 729–739.
(37) Brovelli, F.; Rivas, B. L.; Bernede, J. C. *J. Chilean Chem. Soc.* **2005**, *50*, 597–602.
(38) Tsai, F.-C.; Chang, C.-C.; Liu, C.-L.; Chen, W.-C.; Jenekhe, S. A. *Macromolecules* **2005**, *38*, 1958–1966.
(39) Kiriy, N.; Bocharova, V.; Kiriy, A.; Stamm, M.; Krebs, F. C.; Adler, H.-J. *Chem. Mater.* **2004**, *16*, 4765–4771.
(40) Bourgeaux, M.; Vomscheid, S.; Skene, W. G. *Synth. Commun.* **2007**, *37*, 3551–3558.
(41) Ono, T.; Fujii, S.; Nobori, T.; Lehn, J.-M. *Chem. Commun.* **2007**, 4360–4362.
(42) Giuseppone, N.; Lehn, J.-M. *Chem.—Eur. J.* **2006**, *12*, 1723–1735.

TABLE 1. Comonomer Spectroscopic Data Measured in Anhydrous Acetonitrile

compound	Abs. (nm)[a]	Em. (nm)[b]	Φ_{fl} (10^{-3})[c]	$\Phi_{fl\ (77K)}$[d]	Φ_{ISC}[e]	E_g (eV)[f]	k_r (μs^{-1})[g]	k_{nr} (ns^{-1})[h]	phos. (nm)[i]
1	305	335	2.5	0.009	0.99	3.0	0.19	0.08	479
5[j]	351	422	50.0		0.90	3.2	250	4.8	682
6	457	540	0.38	0.39	0.61	2.2	0.12	0.32	566
7	420	525	0.65	0.21	0.79	2.3	0.31	0.48	552
8	452	535	1.2	0.43	0.57	2.3	0.92	0.77	550
9[k]	440	534	2.8	0.71	0.29	2.3	0.21	0.07	560
10	407[l]	495[m]	27[m]	~0.3[m]	0.15[n]	2.7[o]	20	13	530[n]

[a] Absorption maximum. [b] Emission maximum. [c] Fluorescence quantum yields at λ_{ex} = 303 nm, relative to bithiophene.[28] [d] Fluorescence quantum yields at 77 K relative to room temperature. [e] $\Phi_{ISC} = 1 - \Phi_{fl}$(77 K). [f] Spectroscopic HOMO−LUMO energy gap. [g] $k_r = \Phi_{fl}/\tau_f$. [h] $k_{nr} = k_r(1 - \Phi_{fl})/\Phi_{fl}$. [i] Phosphorescence measured in 4:1 ethanol/methanol glass matrix at 77 K. [j] From Seixas de Melo et al. and Wasserberg et al.[47,48] [k] From Dufresne et al.[28] [l] From Jérôme et al.[49] [m] From Apperloo et al.[50] [n] From Ginocchietti et al.[51] [o] From Frère et al.[52]

be obtained only from **17**. No bisazomethine product was obtained with **16**.

In spite of having to purify the products by column chromatography, the compounds were isolated in reasonable yields. Given the Lewis acid reaction conditions concomitant with the inherent acidic and hydroscopic nature of silica gel that would otherwise hydrolyze labile azomethines, the moderate yields of the comonomers concomitant with the absence of hydrolysis products confirm that the azomethines are robust and stable. The stability of the azomethine bond is evidenced by the lack of reduction with common reducing reagents including $NaBH_4$ and DIBAL. In addition, no decomposition products were observed when exposing the compounds to ambient conditions for prolonged periods of time, which would otherwise hydrolyze moisture and oxygen-sensitive azomethines.[43]

Spectroscopy. The properties of the azomethine derivatives relative to their vinylene carbon analogue (**10**) are seen in Table 1, where a 50 nm bathochromic shift in both the absorption and the fluorescence maximum occurred as a result of the heteroconjugated bond.[44,45] Similarly, a 150 nm absorption bathochromic shift was observed for the comonomers relative to **1**. The same trend was also observed for the fluorescence that is bathochromically shifted by ca. 200 nm relative to **1**. The large spectroscopic shifts are consistent with a highly coplanar π-conjugated structure (vide infra) across which the excited state energy can delocalize efficiently. This is in contrast to homoaryl azomethines whose azomethine mean plane angles are twisted,[46] limiting severely their degree of conjugation.

The absorption and fluorescence spectra provide further information relative to the energy differences between the excited and ground states of the comonomers.[26–28,30] The spectroscopically derived HOMO−LUMO energy gap (E_g) taken from the absorption edge reported in Table 1 for the comonomers is lower than that of their oligothiophene analogue **5** as well as the vinylene analogue **10**. This is a result of the energy levels being effected from the heteroconjugated bond and the electron-withdrawing ester groups. The narrower energy gap and the lower energy levels of the azomethine comonomers imply that the easy condensation method is a suitable means for obtaining conjugated materials with enhanced properties.

Not only do the spectroscopic data provide valuable information regarding the effect of the heteroconjugated bond on the physical properties relative to **10** but they also illustrate the donor strength of the different heterocycles. The effect of the different π-donor groups is seen from the absorption maximum of the comonomers relative to the symmetric all-thiopheno azomethine **9**. Both **6** and **8** are shifted bathochromically by 15 nm relative to **9**. The observed absorption and fluorescence shifts result from the strong π-donor property of the *N*-methyl pyrrole. The azomethines consisting of *N*-methyl pyrrole undergo increased delocalization, resulting in an electronic *push*−*pull* system with the electron-withdrawing esters. The resulting π-donor−donor−acceptor type arrangement promotes intramolecular charge transfer (ICT). The subsequent increased delocalization of the pyrrole azomethine derivatives is evidenced by the absorption bathochromic shifts. Conversely, the poor π-donor properties of the furan heterocycle prevent ICT. This results in a decreased delocalization as evidenced by the 20 nm hypsochromic shift for the absorption and fluorescence spectra of **7** versus **9**.

The weak fluorescence observed from the steady-state emission analyses confirms the comonomers do not dissipate efficiently their singlet excited state by radiative means. This is not surprising since heterocycles such as thiophene and pyrrole are known to deactivate preferentially their singlet excited state by intersystem crossing (ISC) to the triplet state. However, the nonemissive mode of singlet excited state energy dissipation of the azomethine comonomers proceeds differently via internal conversion (IC). This is supported by the 3 orders of magnitude difference between the fluorescence observed in a glass matrix at 77 K relative to that at room temperature (rt; Figure 1). Energy dissipating modes responsible for deactivating the singlet excited state by IC such as bond rotation cannot occur in the low temperature solid matrix. The energy dissipated by IC can therefore be calculated from the fluorescence at different temperatures according to $\Phi_{IC} \approx \Phi_{fl}$(77 K) − Φ_{fl}(rt). The large difference between the nonradiative rate (k_{nr}) and the radiative (k_r) rate constants further corroborates singlet excited state deactivation by IC. It is worthy to note that vinylenes such as **10** also undergo IC; however, their room temperature fluorescence is greater than that of the analogous azomethine derivatives.[50] This implies that deactivation of the excited state by

(43) Wuts, P. G. M.; Greene, T. W. *Greene's Protective Groups in Organic Synthesis*, 4th ed.; Wiley-Interscience: New York, 2007.
(44) Van Der Looy, J. F. A.; Thys, G. J. H.; Dieltiens, P. E. M.; De Schrijver, D.; Van Alsenoy, C.; Geise, H. J. *Tetrahedron* **1997**, *53*, 15069–15084.
(45) An appropriate analogue for direct comparison would be diethyl ester substituted in positions 3 and 4. However, no examples of such a compound are reported.
(46) Skene, W. G.; Dufresne, S. *Org. Lett.* **2004**, *6*, 2949–2952.
(47) Seixas de Melo, J.; Elisei, F.; Becker, R. S. *J. Chem. Phys.* **2002**, *117*, 4428–4435.
(48) Wasserberg, D.; Marsal, P.; Meskers, S. C. J.; Janssen, R. A. J.; Beljonne, D. *J. Phys. Chem. B* **2005**, *109*, 4410–4415.
(49) Jérôme, C.; Maertens, C.; Mertens, M.; Jérôme, R.; Quattrocchi, C.; Lazzaroni, R.; Brédas, J. L. *Synth. Met.* **1996**, *83*, 103–109.
(50) Apperloo, J. J.; Martineau, C.; Hal, P. A. v.; Roncali, J.; Janssen, R. A. J. *J. Phys. Chem. A* **2002**, *106*, 21–31.
(51) Ginocchietti, G.; Galiazzo, G.; Mazzucato, U.; Spalletti, A. *Photochem. Photobiol. Sci.* **2005**, *4*, 547–553.
(52) Frère, P.; Raimundo, J.-M.; Blanchard, P.; Delaunay, J.; Richomme, P.; Sauvajol, J.-L.; Orduna, J.; Garin, J.; Roncali, J. *J. Org. Chem.* **2003**, *68*, 7254–7265.

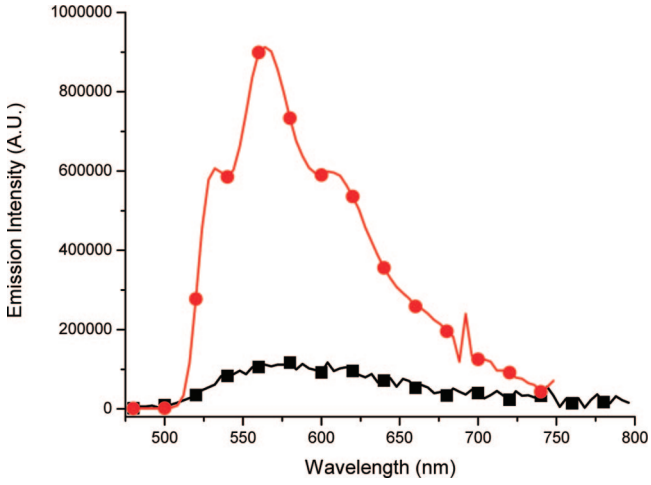

FIGURE 1. Fluorescence of **6** measured at rt (■) and magnified 100 times relative to the fluorescence at 77 K measured in a 4:1 ethanol/methanol glass matrix (●).

rotation around the aryl−CH− and aryl−*N*═ bonds is more efficient for the azomethines than for its corresponding vinylene analogues. The azomethine fluorescence can therefore be modulated by decreasing the temperature, which reduces the modes of deactivation by bond rotation leading to high emission. Similarly, an increase in fluorescence is also expected from the azomethines in the solid state because emission quenching by bond rotation is equally suppressed in this state. The controllable fluorescence is in contrast to oligothiophenes such as **5** that are inherently weak emitters owing to uncontrollable ISC. Consequently, their fluorescence cannot be modulated to obtain high emissions such as with the azomethines.[53]

Even though the low temperature measurements confirm that IC is responsible for the reduced azomethine fluorescence, this deactivation mode does not account entirely for the nonradiative deactivation. This is apparent from summing the Φ_{IC}, calculated from the low temperature fluorescence, and the Φ_{fl} reported in Table 1, which gives less than the expected unity. By substituting the calculated values into the standard energy conservation equation, $\Phi_{fl} + \Phi_{ISC} + \Phi_{IC} \approx 1$, it becomes evident that Φ_{ISC} to the triplet state occurs significantly (0.45) for **6**−**8**. Even though precise measurements of Φ_{IC} are not possible because of the extremely weak fluorescence observed at rt, ISC nonetheless occurs to a higher degree with the different heteroaryl azomethines than for **9**. This is surprising because the reduced number of thiophenes in addition to the preferred azomethine deactivation by IC[47] were expected to decrease the amount of ISC. Although photoisomerization is an additional possible deactivation mode of the singlet excited state, this quenching pathway can be eliminated since no photoisomerization products were observed. The absence of photoisomers is further consistent with the extremely low photoisomerization quantum yield of **10**.[51] Despite the shift in the deactivation mode from IC to ISC, the amount of triplet produced for the π-donor−donor−donor azomethines is consistent with analogous ter-oligofurans and pyrroles consisting of at least one thiophene, whose Φ_{ISC} values are ca. 0.7.[47] The heterocyclic azomethines therefore exhibit triplet properties that are more closely related to their aryl−aryl analogues than their vinylene analogues as a result of lowering of the singlet excited state favoring a $S_1 \rightarrow T_1$ transition.

(53) Becker, R. S.; Seixas de Melo, J.; Maçanita, A. L.; Elisei, F. *J. Phys. Chem.* **1996**, *100*, 18683–18695.

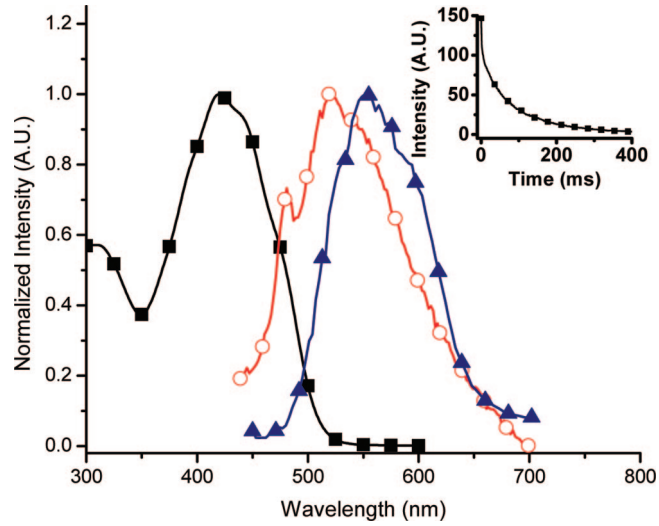

FIGURE 2. Normalized absorption (■) and fluorescence (○) spectra of **7** in acetonitrile. Phosphorescence (▲) spectrum measured in 4:1 ethanol/methanol glass matrix at 77 K. Inset: phosphorescence decay monitored at 552 nm at 77 K.

Phosphorescence measurements were done at 77 K (Figure 2) in order to confirm ISC. The microsecond acquisition times used for these low temperature measurements ensure that the acquired emission spectra are free from fluorescence occurring on the nanosecond time scale. Confirmation of the triplet state formation is further obtained from the low temperature emissions that are bathochromically shifted relative to the fluorescence. To ensure that the observed emissions were assigned correctly to the phosphorescence, the emissions were recorded under the same experimental conditions, but at room temperature instead of a frozen matrix at 77 K. Since the triplet state is rapidly deactivated with diffusion-controlled kinetics at room temperature, the absence of any observable signal at room temperature with the microsecond acquisition confirms that the emission at 77 K is from the triplet. The triplet energies can thus be derived from the 0,0 band where the measured azomethine values are lower than for **10**. The lower triplet energies of **6**−**8** versus that of **10** concomitant with the lower singlet excited state are most likely responsible for the shift in the azomethine deactivation from IC to ISC arising from matching of symmetry allowed $S_1 \rightarrow T_1$ transitions.

Even though the triplet energy can be confirmed by the low temperature measurements, accurate quantification of the triplet state by this simple steady-state method is difficult and is only possible by the time-resolved method of laser flash photolysis (LFP). However, no transient signal was detected by this technique. Given that the LFP time resolution is <100 ns concomitant with the triplet formation confirmed by steady-state studies at 77 K, the absence of transient signal by LFP confirms the triplet states of **6**−**8** are self-quenched, rapidly leading to nonradiative emission.[26–28,30,54] It is well-established that the electrochemically produced amount of triplet versus singlet states is 3:1.[55] The azomethine triplets that would be produced electrochemically in emitting would therefore be efficiently self-quenched, resulting in pristine emission and no delayed emission. The self-quenching concomitant with an expected high fluorescence quantum yield possible by suppress-

(54) Tsang, D.; Bourgeaux, M.; Skene, W. G. *J. Photochem. Photobiol. A* **2007**, *192*, 122–129.
(55) Kobrak, M. N.; Bittner, E. R. *Phys. Rev. B* **2000**, *62*, 11473–11486.

TABLE 2. Selected Comonomer Crystallographic Data

	6[a,b]		**7**[b]		**8**[b]	
	N-methyl pyrrole	thiophene	thiophene	furan	N-methyl pyrrole	furane
plane angle (°)[c]	4.1(1)	4.3(1)	33.6(7)	7.9(2)	18.0(4)	18.7(4)
−C═N− (Å)	1.296(9)	1.279(2)	1.286(4)	1.286(4)	1.287(5)	1.287(5)
═*N*-aryl− (Å)	1.373(2)	1.377(2)	1.381(3)	1.385(3)	1.374(4)	1.374(4)
═CH-aryl− (Å)	1.434(9)	1.436(9)	1.435(4)	1.418(4)	1.419(5)	1.419(5)

[a] From Dufresne et al.[64] [b] Refers to parameters measured between the terminal heterocycle and the central thiophene. [c] Refers to the mean plane angle between the central thiophene and the terminal heterocycle. Values in parentheses refer to uncertainty of measured values.

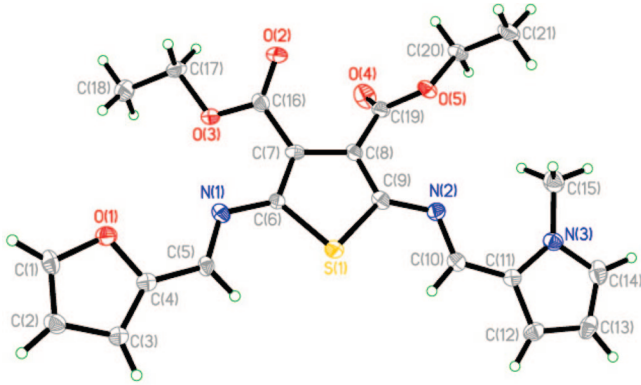

FIGURE 3. ORTEP representation of **8** with the ellipsoids drawn at 30% probability level.

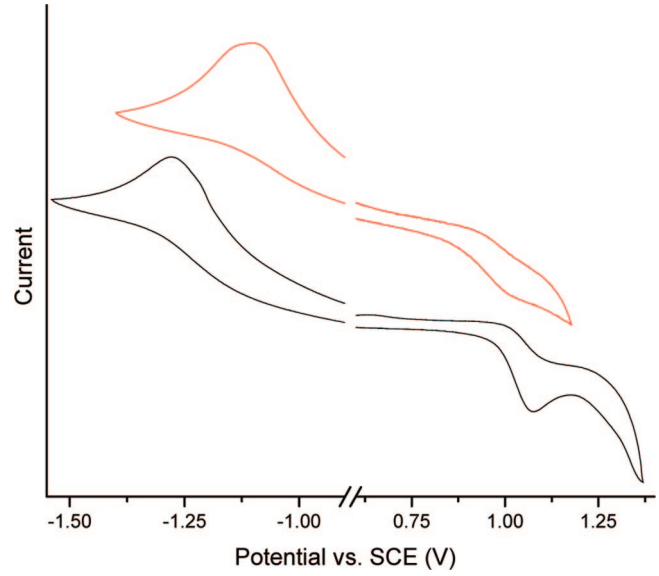

FIGURE 4. Cyclic voltammogram of **8** (black) and **13** (red) measured in anhydrous and deaerated dichloromethane at a scan rate of 100 mV/s with 0.1 M Bu_4NPF_6 of supporting electrolyte.

ing bond rotation deactivation modes possible in the solid state would make the comonomers suitable for functional materials relative to their oligomeric analogues.

X-ray Crystallography. Even though only one isomer was confirmed by ^{1}H NMR for **6**−**8**, absolute assignment to either the *E* or *Z* isomer is not possible by NMR, unlike its carbon analogue. However, the crystal structures obtained for **6**−**8** confirmed that they adopt the *E* isomer. The crystal data also proved that **8** is coplanar with the heteroatoms orientating themselves in an antiparallel arrangement (Figure 3), which is consistent with other azomethines.[56,57,64] The mean planes described by the terminal heterocycles are only twisted slightly from the mean plane described by the central thiophene and the two azomethine bonds to which they are connected (Table 2).[26–28] The observed mean plane angles are in agreement with other heterocyclic azomethines and are in contrast to homoaryl azomethines whose mean planes are highly twisted by 65°.[58] Although **7** and **8** are not entirely coplanar, the compounds are still conjugated through the central thiophene and the two azomethine bonds. Moreover, the spectroscopic data suggest that the compounds are highly conjugated and therefore coplanar in solution. Despite the differences of the mean plane angles between the aryl groups and the azomethine bonds, the C═N, *N*-aryl, and CH−aryl bond distances for **6**−**8** are the same with experimental error. Although the bisazomethines are unsymmetric, the similar bond lengths measured for the two heterocycles in the structure confirm that the compounds are geometrically symmetric. Additionally, the observed coplanarity of the aryl groups and the azomethine bonds validate the high degree of π-conjugation derived from the spectroscopic data.

The crystallographic data also show that intermolecular interactions take place between the comonomers in the solid state. For example, π-stacking occurs between the central thiophene and its complementary terminal pyrrole involving two molecules in different parallel planes that are separated by 3.431(3) Å for **8**. Such interactions contribute to the linear and coplanar configurations adopted by the comonomers. The inherent coplanar and antiparallel configurations of the azomethines are opposite to oligothiophenes, such as **5**, who require steric elements such as long alkyl chains incorporated into their backbone in order to achieve such regioregularity configurations.[59–62] Given that this configuration is partially responsible for the high conductivities and mobilities for oligothiophenes,[63] the inherent coplanarity of the comonomers is expected to also confer similar electrical properties upon doping.

Electrochemistry. Consistent with the oxidation of similar heterocycles, the comonomers underwent an irreversible oxidation corresponding to a one-electron oxidation and formation of the radical cation. In addition to the oxidation process, a reduction process was also observed, as seen in Figure 4. Given the low potential at which the cathodic process occurred combined with the absence of reduced products with standard reductants such as $NaBH_4$ and DIBAL, the electrochemical

(56) Dufresne, S.; Bourgeaux, M.; Skene, W. G. *Acta Crystallogr.* **2006**, *E62*, o5602−o5604.
(57) Skene, W. G.; Dufresne, S.; Trefz, T.; Simard, M. *Acta Crystallogr.* **2006**, *E62*, o2382−o2384.
(58) Skene, W. G.; Dufresne, S. *Acta Crystallogr.* **2006**, *E62*, o1116−o1117.
(59) Iovu, M. C.; Jeffries-El, M.; Zhang, R.; Kowalewski, T.; McCullough, R. D. *J. Macromol. Sci. A: Pure Appl. Chem* **2006**, *43*, 1991–2000.
(60) Iovu, M. C.; Jeffries-El, M.; Sheina, E. E.; Cooper, J. R.; McCullough, R. D. *Polymer* **2005**, *46*, 8582–8586.
(61) Sheina, E. E.; Khersonsky, S. M.; Jones, E. G.; McCullough, R. D. *Chem. Mater.* **2005**, *17*, 3317–3319.
(62) Pan, H.; Liu, P.; Li, Y.; Wu, Y.; Ong, B. S.; Zhu, S.; Xu, G. *Adv. Mater.* **2007**, *19*, 3240–3243.
(63) Roncali, J.; Thobie-Gautier, C. *Adv. Mater.* **1994**, *6*, 846–848.

TABLE 3. Spectroscopic and Cyclic Voltammetry Values for Comonomers and Their Corresponding Polymers

compound	Abs. (nm)[a]	E_{pa}[1] (V)[b]	E_{pc}[1] (V)[c]	HOMO (eV)[d]	LUMO (eV)[d]	E_g[e]
6	457	1.1	−1.3	5.4	3.1	2.3
7	420	1.0	−1.2	5.3	3.2	2.1
8	452	1.1	−1.3	5.4	3.1	2.3
9	440	1.0	−1.3	5.3	3.1	2.2
10[f]	407	0.9		5.2	2.6	2.6
11	483	0.7	−1.1	5.0	3.3	1.7
12	455	0.8	−1.3	5.1	3.1	2.0
13	477	1.0	−1.1	5.3	3.3	2.0
14[g]	466	0.9	−1.0	5.2	3.4	1.8

[a] Absorbance on ITO electrode except for **6**−**8** measured in acetonitrile. [b] Oxidation potential. [c] Reduction potential. [d] Relative to vacuum level. [e] Electrochemical HOMO−LUMO energy gap. [f] From Jérôme et al.[49,67] [g] From Bourgeaux et al.[26,27]

reduction corresponds to the radical anion formation. To ensure that the observed reduction process was not from residual oxygen, the samples were thoroughly deaerated with nitrogen. Meanwhile, oxygen reduction with control experiments in air-saturated solutions occurred at potentials different from those observed in the absence of oxygen. Given the absence of oxygen reduction at −1.43 V (Ag/Ag^+),[65] combined with the 300 mV fluctuation of the reduction potential (E_{pc}) as a function of azomethine structure, the observed cathodic processes are due uniquely to radical anion formation of the comonomers and not to oxygen reduction. The oxidation and reduction onsets can therefore be used to calculate accurately the HOMO and LUMO energy levels, respectively, reported in Table 3 in addition to the energy gaps (E_g) according to standard methods. The consistency between the electrochemically derived E_g and the spectroscopic values validates the electrochemical results. Both methods confirm that the azomethine E_g values are smaller than **10**, confirming the heteroaryl azomethines are more conjugated than their carbon analogues.

Similar to other aryl azomethines and heterocycles, the comonomers studied were oxidized irreversibly owing to the high reactivity of the produced radical cation. The reactivity was exploited for radical cation homocoupling analogous to other heterocycles, resulting in anodically produced films deposited on an ITO electrode. In comparison, homoaryl azomethine comonomers and their corresponding polymers decompose under similar anodic conditions. The bathochromic absorptions of the deposited film relative to the corresponding comonomers (Table 3) confirm that the anodically produced product is more conjugated arising from α−α homocoupling. The conjugated nature of the deposited material is supported further by the measured oxidation potentials of the deposited films that are cathodically shifted by ca. 300 mV relative to the corresponding comonomers as seen in Figure 4. Even though substantially lower oxidation potentials (E_{pa}) of the coupled products relative to their monomers are expected, the increased number of electron-withdrawing ester groups found in the homocoupled products counteract any lowering of the E_{pa} that would otherwise be gained from an increase in the degree of conjugation.[66] Furthermore, radical cation formation of the polymer films derived from **6**−**8** occurs at much lower desired values (≤800 mV) while that for **9** and other polyazomethines occurs at ≥1.0 V. The unsymmetric comonomers are therefore advantageous because their anodically coupled products can be oxidized at lower potentials than their analogues.

Given the unsymmetric nature of the compounds, both *head-to-head* and *head-to-tail* homocoupled products are expected. The spectroscopic and electrochemical data nonetheless provide evidence of anodic coupling of the azomethine-derived comonomers. These represent the first examples of homocoupled azomethine comonomers consisting of various heterocycles. The different sequence of heterocycles in the comonomers additionally offers the means to tailor not only the E_{pa} but also the E_g that can be modulated by 50 kJ/mol. The spectroscopic data also confirm that **6** and **7** have an average degree of polymerization of 6 and 3, respectively, derived from the absorption shifts as a function of the reciprocal degree of conjugation.[31] The low degree of polymerization is responsible for the irreversible oxidation of the anodically produced films, while reversible radical cation is expected with higher molecular weight products. This notwithstanding, the E_{pa} at which the radical cation occurs can be modulated by the heterocycle sequence in the comonomer, while more cathodic potentials are possible with the anodically coupled products relative to their corresponding comonomers. Meanwhile the electrochemical data confirm that both the comonomers and the resulting coupled products can be mutually oxidized and reduced conferring upon them n- and p-doping properties. This implies that the coupled products and their corresponding comonomers can act as mutual charge injectors and acceptors. This is in contrast to their analogues **5** and **10** that can be exclusively oxidized at low potentials and therefore can only be used as hole injection materials.

Conclusion

We have presented the first examples of unsymmetric π-rich conjugated comonomers consisting of thiophene, pyrrole, and furan heterocycles. The versatility of the diaminothiophene **1** to condense selectively with a variety of heteroaryl aldehydes leading to unsymmetric comonomers consisting of different heteroaryl units was possible. This provides a general coupling route for innovative conjugated analogues with tunable photophysical and electrochemical properties. The simple azomethine connections formed during the preparation of these compounds are hydrolytically and reductively robust. The azomethines, however, can be oxidized and reduced to their radical ion intermediates, leading to mutual p- and n-dopable functional materials. The anodically coupled products exhibited more cathodic E_{pa}, confirming their increased degree of conjugation compared to their corresponding comonomers. Furthermore, tunability of the E_{pa} in the anodically produced products is possible via different heterocycles. Despite undergoing a shift from IC to ISC, the rapid and efficient self-quenching of the triplet state afforded pristine emission while the fluorescence yield can be controlled by external parameters such as temperature.

Experimental Section

Synthesis. 2,5-Diaminothiophene-3,4-dicarboxylic acid diethyl ester (1). The synthesis was done according to previous reports.[40]

Diethyl 2-((furan-2-yl)methyleneamino)-5-aminothiophene-3,4-dicarboxylate (15). 2 (37 mg, 0.39 mmol) and **1** (100 mg, 0.39 mmol) were mixed in anhydrous isopropanol with a catalytic amount of TFA and refluxed for 12 h. The reaction was then purified by flash chromatography (SiO_2) eluted with 90/10 hexanes/ethyl

(64) Dufresne, S.; Skene, W. G. *Acta Crystallogr.* **2008**, *E64*, 1.
(65) *Handbook of Chemistry & Physics*, *88* ed.; CRC: Boca Raton, FL, 2007.
(66) We demonstrated previously with 3,4-dialkylated comonomers that α−α coupling is produced exclusively. See ref 31.
(67) Jérôme, C.; Maertens, C.; Mertens, M.; Jérôme, R.; Quattrocchi, C.; Lazzaroni, R.; Brédas, J. L. *Synth. Met.* **1997**, *84*, 163–164.

acetate up to 60/40 hexanes/ethyl acetate to afford 110 mg (85%) of a brownish yellow solid: mp 151−153 °C; ^{1}H NMR (acetone-d_6) δ 7.92 (s, 1H), 7.75 (d, 1H, J = 1.3 Hz), 7.50 (s, NH_2), 6.97 (d, 1H, J = 3.4 Hz), 6.63 (dd, 1H, ^3J = 3.4 and 1.6 Hz); ^{13}C NMR (acetone-d_6) δ 165.0, 164.3, 161.1, 152.6, 146.1, 140.7, 133.3, 130.8, 115.3, 112.8, 102.0, 61.0, 60.0, 14.1, 14.1; HRMS(+) calcd for $[C_{15}H_{16}N_2O_5S+H]^+$ 337.08527, found 337.08535.

Diethyl2-((thiophen-2-yl)methyleneamino)-5-aminothiophene-3,4-dicarboxylate (17). To a 50 mL round-bottom flask was added **1** (50 mg, 0.19 mmol) in absolute ethanol (20 mL) to which was added **3** (24 mg, 0.21 mmol) and a catalytic amount of trifluoroacetic acid (TFA). The mixture was refluxed for 20 h under normal atmosphere. Complete removal of the solvent led to an orange solid which was purified by flash chromatography (SiO_2) and eluted with 80/20 hexanes/ethyl acetate. The product was isolated as an orange solid (81%): mp 114−116 °C; ^{1}H NMR (acetone-d_6) δ 8.24 (s, 1H), 7.63 (d, 1H, J = 5.0 Hz), 7.52 (dd, 1H, J = 3.7 and 0.7 Hz), 7.48 (s, 2H), 7.14 (dd, 1H, J = 5.0 and 3.7 Hz), 4.32 (q, 2H, J = 7.2 Hz), 4.19 (q, 2H, J = 7.1 Hz), 1.37 (t, 3H, J = 7.1 Hz), 1.26 (t, 3H, J = 7.1 Hz); ^{13}C NMR (acetone-d_6) δ 165.0, 164.3, 161.1, 161.0, 146.1, 143.2, 132.8, 132.1, 130.5, 128.4, 101.8, 61.0, 60.0, 14.3, 14.1; HRMS(+) calcd for $[C_{15}H_{16}O_4N_2S_2+H]^+$ 353.06242, found 353.06251.

Diethyl2-((1-methyl-1*H*-pyrrol-2-yl)methyleneamino)-5-((thiophen-2-yl)methyleneamino)thiophene-3,4-dicarboxylate (6). To a 50 mL round-bottom flask was added **4** (40 mg, 0.37 mmol) dissolved in anhydrous toluene (25 mL) to which was subsequently added DABCO (159 mg, 1.42 mmol) and 1.0 M $TiCl_4$ solution in toluene (0.28 mL, 0.28 mmol) at 0 °C, and then **17** (100 mg, 0.28 mmol) was added. The mixture was then refluxed for 4 h after which the solvent was removed. Purification by flash chromatography (SiO_2) with 30/70 ether/hexanes, switched to 70/30 hexanes/ethyl acetate and then increased up to 50/50 hexanes/ethyl acetate to yield the title product as a red solid (63 mg, 50%): mp 112−114 °C; ^{1}H NMR (acetone-d_6) δ 8.68 (s, 1H), 8.35 (s,1H), 7.80 (d, 1H, J = 4.9 Hz), 7.72 (d, 1H, J = 3.7 Hz), 7.23 (dd, 1H, J = 4.9 Hz and 3.7 Hz), 7.14 (m, 1H), 6.87 (q, 1H, J = 4.0 and 1.8 Hz), 6.24 (q, 1H, J = 4.0 and 2.5 Hz), 4.32 (q, 2H, J = 7.0 Hz), 4.28 (q, 2H, J = 7.2 Hz), 4.07 (s, 3H), 1.37 (t, 3H, J = 7.1 Hz), 1.31 (t, 3H, J = 7.0 Hz); ^{13}C NMR (acetone-d_6) δ 163.5, 163.0, 152.2, 152.2, 150.3, 146.6, 142.6, 134.5, 132.6, 132.6, 129.9, 128.9, 128.8, 124.9, 122.4, 110.1, 61.1, 61.0, 37.0, 14.2, 14.0; HRMS(+) calcd for $[C_{21}H_{21}N_3O_4S_2+H]^+$ 444.10462, found 444.10396.

Diethyl 2-((furan-2-yl)methyleneamino)-5-((thiophen-2-yl)-methyleneamino)thiophene-3,4-dicarboxylate (7). To a 50 mL round-bottom flask was added **3** (27 μL, 0.29 mmol) dissolved in anhydrous toluene (25 mL) to which was subsequently added DABCO (125 mg, 1.11 mmol) and 1.0 M $TiCl_4$ solution in toluene (0.29 mL, 0.29 mmol) at 0 °C, and then **15** (75 mg, 0.22 mmol) was added. The mixture was then refluxed for 4 h after which the solvent was then removed. Purification by flash chromatography (SiO_2) with 50/50 ether/hexanes and 1% triethylamine, switched to 70/30 hexanes/ethyl acetate and then increased up to 50/50 hexanes/ethyl acetate with 1% NEt_3 to yield the title product as a red solid (79 mg, 83%): mp 133−135 °C; ^{1}H NMR (acetone-d_6) δ 8.75 (s, 1H), 8.38 (s,1H), 7.89 (d, 1H, J = 1.4 Hz), 7.85 (d, 1H, J = 5.0 Hz), 7.77 (dd, 1H, J = 3.8 and 0.8 Hz), 7.25 (q, 1H, J = 5.0 and 3.7 Hz), 7.24 (d, 1H, J = 3.6 Hz), 6.73 (dd, 1H, J = 3.5 and 1.8 Hz), 4.32 (q, 2H, J = 7.1 Hz), 4.30 (q, 2H, J = 7.1 Hz), 1.36 (t, 3H, J = 7.2 Hz), 1.33 (t, 3H, J = 7.2 Hz); ^{13}C NMR (acetone-d_6) δ 163.0, 153.7, 152.1, 149.5, 147.9, 147.7, 146.1, 142.4, 140.6, 135.1, 133.2, 128.9, 127.8, 127.3, 119.0, 113.4, 61.2, 61.2, 14.2, 14.0; HRMS(+) calcd for $[C_{20}H_{18}N_2O_5S_2+H]^+$ 431.07299, found 431.07201.

Diethyl 2-((1-methyl-1*H*-pyrrol-2-yl)methyleneamino)-5-((furan-2-yl)methyleneamino)thiophene-3,4-dicarboxylate (8). To a 50 mL round-bottom flask was added **4** (32 mg, 0.29 mmol) dissolved in anhydrous toluene (25 mL) to which was subsequently added DABCO (125 mg, 1.11 mmol) and 1.0 M $TiCl_4$ solution in toluene (0.29 mL, 0.29 mmol) at 0 °C, and then **15** (75 mg, 0.22 mmol) was added. The mixture was then refluxed for 4 h after which the solvent was removed. Purification by flash chromatography (SiO_2) with 30/70 ether/hexanes and 1% triethylamine, switched to 70/30 hexanes/ethyl acetate and then increased up to 50/50 hexanes/ethyl acetate with 1% NEt_3 to yield the title product as a red solid (45 mg, 47%): mp 110−114 °C; ^{1}H NMR (acetone-d_6) δ 8.36 (s, 1H), 8.33 (s,1H), 7.86 (d, 1H, J = 1.5 Hz), 7.20 (d, 1H, J = 3.5 Hz), 7.14 (m, 1H), 6.88 (q, 1H, J = 3.9 and 1.5 Hz), 6.71 (q, 1H, J = 3.6 and 1.8 Hz), 6.25 (q, 1H, J = 3.9 and 2.6 Hz), 4.31 (q, 2H, J = 7.1 Hz), 4.28 (q, 2H, J = 7.2 Hz), 4.09 (s, 3H), 1.34 (t, 3H, J = 7.0 Hz), 1.31 (t, 3H, J = 7.0 Hz); ^{13}C NMR (acetone-d_6) δ 163.5, 163.0, 152.5, 152.3, 150.4, 147.6, 146.9, 146.3, 132.7, 129.9, 129.2, 124.9, 122.4, 118.3, 113.3, 110.1, 61.1, 61.0, 37.0, 14.1, 14.0; HRMS(+) calcd for $[C_{21}H_{21}N_3O_5S+H]^+$ 428.12747, found 428.12668.

TABLE 4. Details of Crystal Structure Determination for 8

formula	$C_{21}H_{21}N_3O_5S$
Mw(g/mol); F(000)	427.47; 896
crystal color and form	red plate
crystal size (mm)	0.15 × 0.09 × 0.05
T (K); d_{calcd} (g/cm^3)	150(2); 1.407
crystal system	monoclinic
space group	$P2_1/c$
unit cell: a (Å)	15.041(3)
b (Å)	7.5421(15)
c (Å)	18.827(4)
α (°)	90.000
β (°)	109.17(3)
γ (°)	90.000
V (Å^3); Z	2017.4(8); 4
θ range (°); completeness	3.11−72.07; 0.960
reflections: collected/independent; R_{int}	19643/3816 0.147
μ (mm^{-1}) Abs. Corr.	1.767 semiempirical
$R1(F)$; $wR(F^2)$ [$I > 2\sigma(I)$]	0.0775; 0.1560
$R1(F)$; $wR(F^2)$ (all data)	0.1529; 0.1875
GoF (F^2)	0.955
max. residual e$^-$ density	−0.504 e$^-$·Å^{-3}

Crystal Structure Determination. Diffraction data for **6** were collected on a diffractometer using graphite-monochromatized Cu Kα radiation with 1.54178 Å. The structures were solved by direct methods (SHELXS97). All non-hydrogen atoms were refined based on Fobs2 (SHELXS97), while hydrogen atoms were refined on calculated positions with fixed isotropic U, using riding model techniques.

Diffraction data for **8** (Table 4) were collected on a Bruker FR591 diffractometer using graphite-monochromatized Cu Kα radiation with 1.54178 Å. The structures were solved by direct methods (SHELXS97). All non-hydrogen atoms were refined based on Fobs2 (SHELXS97), while hydrogen atoms were refined on calculated positions with fixed isotropic U, using riding model techniques.

Acknowledgment. The authors acknowledge financial support from the Natural Sciences and Engineering Research Council Canada, and the Centre for Self-Assembled Chemical Structures. Appreciation is extended Prof. D. Zargarian for helpful discussions, and to Joao-Nicolas Blair-Pereira. S.D. thanks the Université de Montréal for a graduate scholarship.

Supporting Information Available: ^{1}H and ^{13}C spectra of **6**−**8**, **15**, and **17**, absorption and emission spectra of **6**−**8**, cyclic voltammograms of **6**−**8** and **11**−**13**, and CIF files for **7** and **8**. This material is available free of charge via the Internet at http://pubs.acs.org.

JO8002503